Oncogene homologue Sch9 promotes age-dependent mutations by a superoxide and Rev1/Polζ-dependent mechanism

Federica Madia,[1] Min Wei,[1] Valerie Yuan,[1] Jia Hu,[1] Cristina Gattazzo,[1] Phuong Pham,[2] Myron F. Goodman,[2] and Valter D. Longo[1]

[1]Andrus Gerontology Center and Department of Biological Sciences, and [2]Molecular and Computational Biology, Department of Biological Sciences, University of Southern California, Los Angeles, CA 90089

Oncogenes contribute to tumorigenesis by promoting growth and inhibiting apoptosis. Here we examine the function of Sch9, the *Saccharomyces cerevisiae* homologue of the mammalian Akt and S6 kinase, in DNA damage and genomic instability during aging in nondividing cells. Attenuation of age-dependent increases in base substitutions, small DNA insertions/deletions, and gross chromosomal rearrangements (GCRs) in *sch9Δ* mutants is associated with increased mitochondrial superoxide dismutase (MnSOD) expression, decreased DNA oxidation, reduced *REV1* expression and translesion synthesis, and elevated resistance to oxidative stress-induced mutagenesis. Deletion of *REV1*, the lack of components of the error-prone Polζ, or the overexpression of *SOD1* or *SOD2* is sufficient to reduce age-dependent point mutations in *SCH9* overexpressors, but *REV1* deficiency causes a major increase in GCRs. These results suggest that the proto-oncogene homologue Sch9 promotes the accumulation of superoxide-dependent DNA damage in nondividing cells, which induces error-prone DNA repair that generates point mutations to avoid GCRs and cell death during the first round of replication.

Introduction

Mutations that activate the Akt and Ras proto-oncogenes or the upstream insulin-like growth factor 1 (IGF-I) receptor are among the most frequently detected in human cancers (Rodriguez-Viciana et al., 1994, 2005; Toker and Yoeli-Lerner, 2006). Because of their roles in stimulating cellular proliferation and inhibiting apoptosis, these oncogenes are widely believed to contribute to cancer by allowing damaged cells to survive, grow, and metastasize (DePinho, 2000; Pollak et al., 2004; Anisimov et al., 2005; Toker and Yoeli-Lerner, 2006). Mutations that cause the down-regulation of homologues of Ras, Akt, or IGF-I receptors extend life spans in organisms ranging from yeast to mice (Longo and Finch, 2003), and deficiency in IGF-I or IGF-I–like signaling (IIS) is associated with decreased neoplastic death in mice (Vergara et al., 2004; Anisimov et al., 2005) or resistance to germline tumors in *Caenorhabditis elegans* (Pinkston et al., 2006). In agreement with the widely accepted role for IGF-I, Akt, and Ras in cancer, Pinkston et al. (2006) proposed that the resistance of the *C. elegans* daf-2/insulin-receptor mutants to gld-1–dependent germline tumors is attributed to decreased cell division and increased apoptosis within the tumors. Although defects in cell division and apoptosis undoubtedly play a major role in mutagenesis and cancer, our previous studies in *Saccharomyces cerevisiae* provided evidence for a link between Sch9, homologue of mammalian S6K and Akt (Toda et al., 1988; Urban et al., 2007), and age-dependent spontaneous mutations in nondividing yeast cells (Fabrizio et al., 2004, 2005), which raises the possibility that proto-oncogene homologues may contribute to DNA damage during aging independently of cell division (Lombard et al., 2005).

The present study investigates the mechanisms underlying the role of Sch9 in increasing DNA damage and genomic

Correspondence to Valter D. Longo: vlongo@usc.edu

Abbreviations used in this paper: 5FOA, 5-fluoroorotic acid; 8-OHdG; 8-hydroxy-2′ deoxyguanidine; ANOVA, analysis of variance; CFU, colony-forming unit; GCR, gross chromosomal rearrangement; IGF-I, insulin-like growth factor 1; MMS, methyl methane sulfonate; SDC, synthetic dextrose complete; SOD, superoxide dismutase; TLS, translesion synthesis.

The Rockefeller University Press $30.00
J. Cell Biol. Vol. 186 No. 4 509–523
www.jcb.org/cgi/doi/10.1083/jcb.200906011

instability. We present data indicating that, in chronologically aging yeast, DNA damage occurs primarily in quiescent cells. The deletion of the proto-oncogene homologue *SCH9* postpones/attenuates age-dependent mutagenesis by up-regulating the transcription factor Gis1, increasing the expression of mitochondrial *SOD2*, preventing superoxide-dependent DNA oxidation, and reducing the expression of *REV1* and translesion synthesis (TLS) activity. We propose that both superoxide and the error-prone Rev1/Polζ-dependent TLS are required for the major portion of age-dependent mutations.

Results

Sch9 promotes age-dependent genomic instability

The yeast chronological life span (Fabrizio and Longo, 2003, 2007) has provided a paradigm for the identification of key pathways responsible for the regulation of life span and age-dependent damage (Fabrizio et al., 2001). The combination of this simple model organism with several mutator assays (Madia et al., 2007) has proven to be a valuable system to address the mechanisms underlying age-dependent genomic instability.

Using the canavanine resistance assay (Can^r), which detects mutations that abolish *CAN1* function (Chen and Kolodner, 1999), we have previously reported that chronologically aging yeast displayed a progressive increase of spontaneous mutation frequency (Fabrizio et al., 2004). More recently, we demonstrated that this age-dependent increase of genomic instability encompassed various categories of mutations: gross chromosomal rearrangements (GCRs; Can^r5FOA^r), point mutations (*trp1-289* reversions, $trp^- \rightarrow Trp^+$) and small insertion/deletion mutations (*lys2-BglII* $\rightarrow Lys^+$; Madia et al., 2008). The deletion of *SCH9* not only extends life span (Fig. 1 A) but also attenuates/delays the age-dependent increase in spontaneous Can^r mutation frequency (Fig. 1 B; Fabrizio et al., 2004, 2005) and prevents the premature genomic instability caused by the Sgs1 helicase deficiency (Madia et al., 2008).

Given the homology to the mammalian AKT and S6K and their implication in tumorigenesis, we investigated the role of Sch9 in the regulation of genomic instability and the mechanism linking its activity to DNA mutations. We determined the cumulative number of Can^r mutations from day 1 to day 7 in the wild type and to day 15 in *sch9Δ* cells, which represent the ∼50% survival point of each population, respectively (Fig. 1 C). The data indicated that in *SCH9*-deficient cells, the protection against the generation of age-dependent mutations was not simply the result of postponed mortality ($P = 0.0013$, cumulative Can^r mutations in the wild type on day 7 vs. *sch9Δ* on day 15; Fig. 1 C). Consistent with the observed low amount of Can^r mutations (Fig. 1 B), the deletion of *SCH9* caused a significant reduction (10-fold compared with wild-type cells) in GCRs over the 13-d period of a chronological life span study (Fig. 1 D). Notably, only ∼1% of the wild-type cells survived to day 13 (Fig. 1 A), which indicates that GCRs are very high in the small subpopulation of old cells that survived to advanced ages.

We then extended the analysis to other types of DNA lesions by examining the occurrence of a specific single base-substitution mutation (T to C: *trp1-289* reversions, $trp^- \rightarrow Trp^+$; Capizzi and Jameson, 1973) and small insertion/deletion mutations (*lys2-BglII* $\rightarrow Lys^+$); the latter may serve as an indicator for nonhomologous end-joining activity (Heidenreich and Wintersberger, 1998; Heidenreich et al., 2003). Interestingly, *SCH9*-deficient cells displayed a twofold reduction of single point mutations (Fig. 1 E) as well as a fivefold reduction of the frequency of small DNA insertion/deletion (Lys^+) mutations compared with wild-type cells (Fig. 1 F). The results presented in Fig. 1 (A–F) suggest that the lack of *SCH9* protects chronologically aging yeast cells against a wide variety of mutations.

SCH9 deletion enhances G1 arrest and reduces age-dependent regrowth

The inability to properly exit the cell cycle can lead to senescence and cancer (Campisi, 2001), and can contribute to mutagenesis. Our previous studies and those from other laboratories suggest that life span–extending mutations cause a switch from a pro-growth to a pro-maintenance mode (Longo, 2003). To determine whether the *sch9Δ* mutation increases protection against age-dependent genomic instability by promoting G1 arrest, we assessed cell cycle profiles and budding indices of wild-type and *sch9Δ* mutants. The deletion of *SCH9* indeed reduced the budding index from ∼2–3% to 1% on days 3, 5, and 7 (Fig. 1 G). FACS analysis confirmed that *sch9Δ* cells (98% of the population, starting from day 1) were arrested in the G1 phase (Figs. 1 H and S1 A). Notably, the low budding index as well as the high percentage of G1 arrested cells in *sch9Δ* cultures are in agreement with our earlier work indicating that deletion of *SCH9* caused a major reduction in age-dependent "regrowth," which appears to depend on adaptive mutations and resembles the differentiation process that leads to tumorigenesis in mammalian cells (Fabrizio et al., 2003, 2004, 2005). The age-dependent early regrowth frequency (days 7–17; Madia et al., 2008) in a large number of cultures of three different genetic backgrounds confirmed that mutants lacking *SCH9* were unable to regrow, whereas wild-type populations display the regrowth phenomenon (Table S1).

Quiescent cells contribute to age-dependent mutagenesis

The inability of aging cells to properly arrest in G1 could lead to a higher mutation frequency (Bartkova et al., 2005; Houtgraaf et al., 2006; Burhans and Weinberger, 2007; Löbrich and Jeggo, 2007). Sch9 may increase mutations during chronological aging by promoting replication and cell division before the cell is able to repair DNA damage, causing "replication stress" (Weinberger et al., 2007). To test this possibility, we isolated quiescent and nonquiescent cells from cultures aging chronologically using the Percoll density gradient fractionation (Fig. 2 A; Allen et al., 2006; Aragon et al., 2008; Madia et al., 2008). This method allowed the separation of two distinct subpopulations: the upper fraction, mainly composed of a heterogeneous population of nonquiescent cells, including dividing mother cells, nondividing, apoptotic, and necrotic cells; and a lower fraction mainly composed of

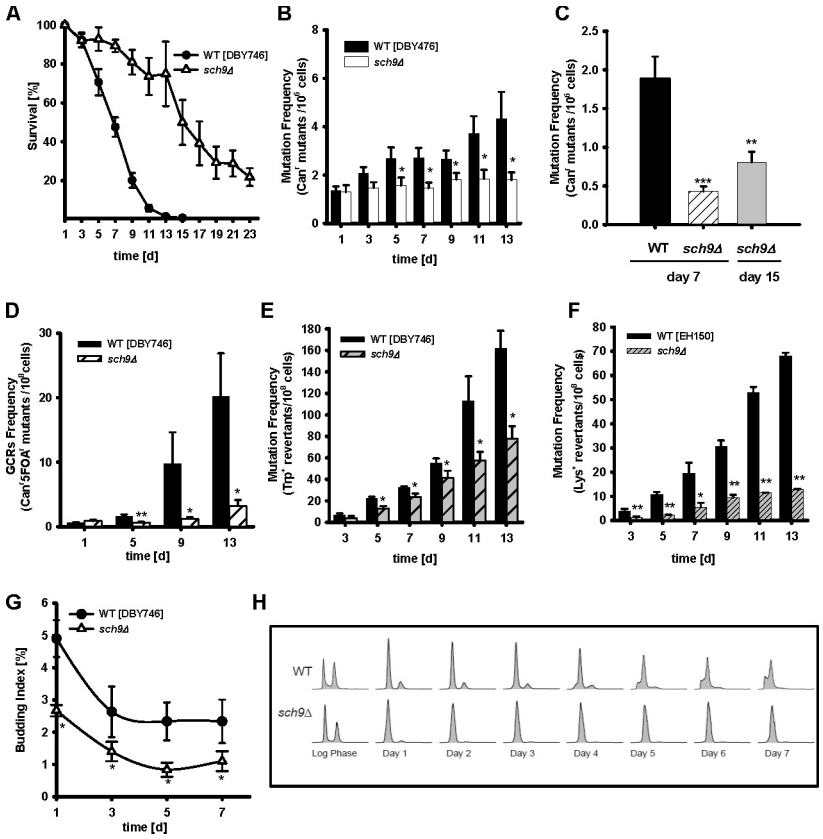

Figure 1. **Attenuated age-dependent genomic instability in cells lacking the oncogene homologue *SCH9*.** (A) Chronological survival. Data represent the mean ± SEM (error bars), $n = 12–14$. (B) Mutation frequency over time in the *CAN1* gene (measured as Can^r mutants/10^6 cells, $n = 20$). (C) Cumulative mutation frequency, measured as Can^r mutants/10^6 cells, calculated from day 1 to day 7 or to day 15 in the wild type (DBY746) and mutants lacking *SCH9*. Day 7 and day 15 represent the ∼50% survival point of the wild type and *sch9Δ* population, respectively. $n = 20$. **, $P < 0.01$; ***, $P < 0.001$; ANOVA test, Tukey's test versus wild type (WT) on day 7. (D) GCR frequency (Can^{r}5FOA^r mutants/10^8 cells, $n = 10–11$). (E) Age-dependent base substitutions (*trp1-289* reversion) frequency ($n = 8–9$). (F) Small DNA insertion/deletion mutations in the *lys*ΔBglII background (EH150 strains, $n = 8–9$). (G) Budding index of chronologically aging cells ($n = 6$). (H) Cell cycle profile (FACS) during chronological aging. Strains shown are wild type (DBY746) and *sch9*Δ. Data represent the mean ± SEM (error bars). *, $P < 0.05$; **, $P < 0.01$; ***, $P < 0.001$; two-tailed *t* test, *sch9*Δ versus WT at the indicated time points.

quiescent cells (Fig. 2, A and B; and Fig. S1 B; Allen et al., 2006; Aragon et al., 2008). The budding indices were also measured in both the quiescent and nonquiescent cell fraction (Fig. 2 D).

On day 3, 60% of wild-type cells were in the upper nonquiescent fraction (Fig. 2 C). This fraction increased gradually from day 3 to day 7. Interestingly, the Can^r mutation frequency in the nonquiescent wild-type subpopulation was significantly lower than that in the quiescent subpopulation (Fig. 2 E). Furthermore, the frequency of mutations in the nonquiescent subpopulation remained unchanged over time, whereas an age-dependent increase of mutations was observed in the quiescent fraction ($P < 0.05$: day 7 vs. day 3; Fig. 2 E). This result indicates that quiescent cells may accumulate DNA damage that leads to mutations. In contrast to the wild type, *SCH9*-deficient cells were mostly quiescent, as indicated by FACS analysis (Figs. 1 H and S1 B). From day 3 to day 7, >90% of the *SCH9*-deficient cells separated in the lower fraction compared with 10–40% of wild-type cells (Fig. 2 C). The deletion of *SCH9* caused a decrease of mutation frequency in the quiescent fraction compared with that of wild type, and abolished the age-dependent increase in mutations (Fig. 2 E). The latter data suggest that the effect of *SCH9* deletion on the cell cycle state does not play a major role in age-dependent mutations.

To test whether mutations may occur during the multiple rounds of cell divisions required to generate a colony and not during either the aging of the nondividing population or the very first round of replication, we allowed old wild-type and *sch9Δ* cells to undergo one population doubling before treatment with the toxic L-canavanine sulfate. If the DNA damage did not occur during aging but during multiple rounds of cell division after exit from G_0, we would expect the additional population doubling of the 2×10^7 cells to cause a major increase in mutation frequency. The frequency of mutations normalized for population size, instead, remained the same for cells exposed to canavanine before or after one population doubling (Fig. 2 F), which suggests that at least the initial DNA damage in the *CAN1* gene occurs in the nondividing cells.

Gis1, a stress-response transcription factor downstream of Sch9, regulates the expression of *REV1* and DNA mutations

The anti-aging and stress-resistance effects of the *sch9Δ* mutations depend on the protein kinase Rim15 and its downstream stress response transcription factors Gis1, Msn2, and Msn4 (Fabrizio et al., 2001, 2003; Wei et al., 2008). Deficiency in Gis1 led to an elevation of mutation frequency in the wild type (Fig. 3 B) and reversed the protective effect of *sch9Δ* on age-dependent mutations starting from day 9 (Fig. 3, A and B). To investigate further the mediators of the Sch9 effect on DNA mutations, we obtained the global gene expression profiles of 2.5-d-old *sch9Δ* and wild-type cells. Among the DNA repair genes, *REV1*, encoding the deoxycytidyl transferase that is involved in TLS and the repair of abasic sites, and the recombination repair genes *RAD51* and *RAD54* were among the most down-regulated (Fig. 3 C and Table S2) in the long-lived *sch9Δ* mutants.

REV1 mRNA level was 40% lower in *sch9Δ* mutant cells compared with wild-type cells on day 3 (Fig. 4 A). Deletion of

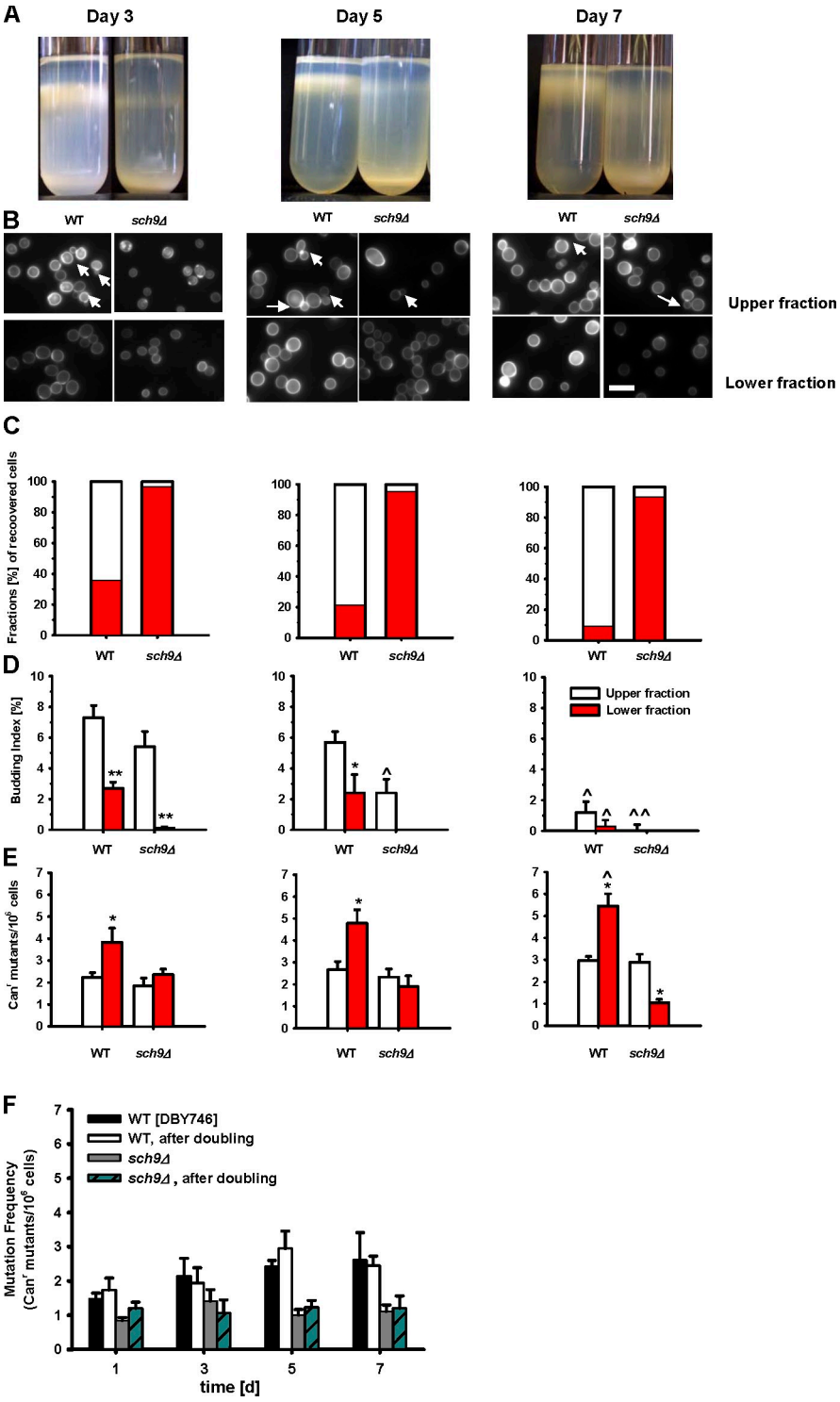

Figure 2. **Genomic instability arises from quiescent cells during chronological aging.** (A) Density-gradient separation of nonquiescent (upper) and quiescent (lower) cells from chronologically aging cultures. (B) Calcofluor staining of upper and lower fractions from wild-type and *sch9*Δ mutant cultures. The arrows indicate budding cells. Bar, 10 µm. (C) Percentage of upper and lower fractions in the culture. (D) Budding indices of upper and lower fractions (n = 6–7). (E) Mutation frequency in *CAN1* gene (Can^r mutants/10^6 cells) in the upper and lower fractions (n = 6–7). (F) Mutation frequency in the *CAN1* gene before and after allowing the cells to undergo one population doubling during a standard chronological life span study (n = 4). Error bars indicate ±SEM. (C–E) Data represent the mean ± SEM (error bars); *, P < 0.05; **, P < 0.01; two-tailed t test, *sch9*Δ versus wild type (WT). ^, P < 0.05; ^^, P < 0.01; two-tailed t test, day 5 or day 7 versus day 3 of the same strain.

GIS1 in both wild-type and *sch9Δ* mutant cells was associated with significant increase in the *REV1* mRNA level (Fig. 4 A), suggesting that Sch9 modulates Rev1 expression/activity partially through the down-regulation of the transcription factor Gis1. However, the deletion of *SCH9* caused a major reduction of *REV1* expression and of mutation frequency during the first 7 d of survival even in *GIS1*-deficient cells, which suggests that part of the protective effect is Gis1 independent. Other transcription factors such as Msn2 and Msn4 activated in *sch9Δ* mutants might be partially responsible for the effect on life span and mutations (Fig. 3, A and B).

The Y superfamily DNA polymerase Rev1 and Polζ mediate Sch9-dependent mutations during aging

To gain further insight into the types of age-dependent mutations, we analyzed the mutation spectra in Can^r mutant colonies arising from chronologically aging wild-type and *sch9Δ* cultures

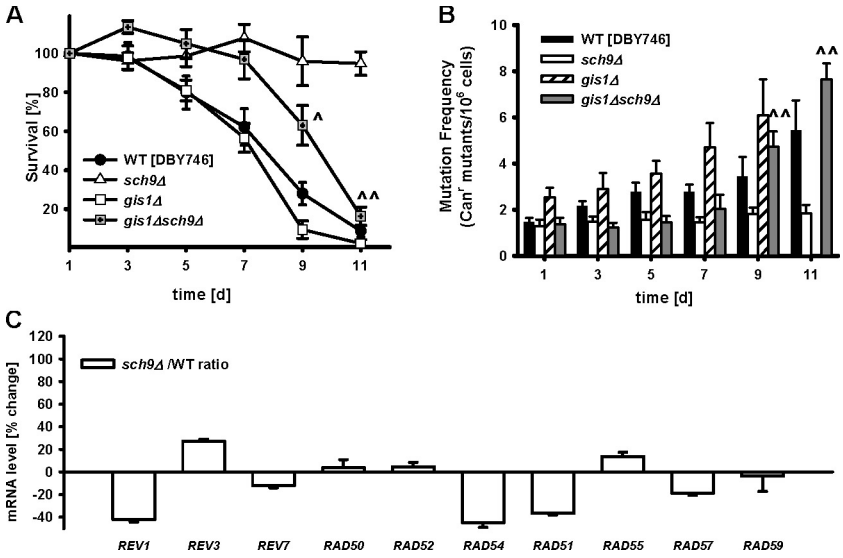

Figure 3. **Stress response transcription factor Gis1 is required for life span extension and attenuated genomic instability associated with *SCH9* deficiency.** (A) Chronological survival (n = 11) and (B) mutation frequency in the *CAN1* gene (n = 11) of the wild type (WT; DBY746) and *sch9*Δ mutants. ^, $P < 0.05$; ^^, $P < 0.01$; two-tailed t test, *sch9*Δ *gis1*Δ versus *sch9*Δ at the indicated time points. (C) mRNA levels of *REV1*, *REV3*, *REV7*, and recombination genes involved in DNA repair. WT (DBY746) and *sch9*Δ were grown in SDC media. Cells were collected on day 2.5 for mRNA extraction and microarray analysis. Data represent mean ± SEM (error bars) of percentage change, *sch9*Δ versus WT (n = 3). For complete microarray data, see Table S2.

on day 7, when the difference in mutation frequency was elevated and 50% of the wild-type population was still alive (Fig. 1 C and Table I). Sequencing data of Can^r mutants from wild-type cultures indicated a high occurrence of multiple mutations within a short stretch of a 500–1,000-bps DNA sequence (6 out of 10 mutated *CAN1* genes): base substitutions accompanied with frameshift mutations caused by small deletion or insertion of homopolymeric runs (sequences of 3–4 or more identical nucleotides, often As and/or Ts; Table I). In agreement with the age-dependent increase in oxidative stress (Moraes et al., 1990; Kreutzer and Essigmann, 1998; Wang et al., 1998), we observed a high occurrence of G → T (transversion) or C → T (transition) mutations in wild-type cells, which was not seen in the *sch9Δ* cells (Table I). It is not clear why 5 out of 10 sequenced *CAN1* genes from *sch9Δ* mutant colonies contained a C → A base substitution at position 11 away from ATG (Table I). One possibility is that this base may constitute a mutation hot spot. Another possibility is that the mutation generated during the growth phase expanded with the population. Multiple mutational events were not observed in cells lacking *SCH9*. Only 2 out of 10 Can^r mutants from *sch9Δ* cultures contained multiple substitution/deletion/insertion mutations on day 7 (Table I).

The mutation pattern observed in wild-type cells was consistent with the recruitment to the DNA lesion site of error-prone polymerases, which is analogous to SOS-induced mutagenesis in *Escherichia coli* mediated by PolIV and PolV of the Y superfamily of polymerases (Tang et al., 2000; Kobayashi et al., 2002). This family includes Rev1 and Rad30 (Polη) in *S. cerevisiae* (Ohmori et al., 2001). Most spontaneous and damage-induced mutagenesis during growth phase was found to depend on Rev1 and the DNA polymerase zeta (Polζ, which belongs to the B superfamily of DNA polymerases; Quah et al., 1980). Sloppy DNA synthesis by error-prone polymerases could then have been responsible for the multiple mutations observed in the aging wild-type cells (Table I). The absence of multiple mutation events in the *CAN1* gene in 7-d-old *rev1Δ* mutants (Table I) suggests a role for Rev1 in the sloppy DNA synthesis leading to the secondary mutations.

Considering that *REV1* was among the most down-regulated DNA repair-related genes in *sch9Δ* (Fig. 3 C and Table S2) and that its mRNA expression was significantly increased in the absence of the downstream Sch9 effector Gis1 (Fig. 4 A), we tested whether the Rev1 protein mediated the effect of Sch9 on age-dependent genomic instability. In the DBY746 background, spontaneous age-dependent mutation frequency started at a much lower level and did not increase in cells lacking *REV1* (Fig. 4 C). Similar results were obtained in the BY4741 background (Fig. 4, B and C). *rev1Δ* cells died earlier than wild-type cells in the DBY746 (Fig. 4 B) but not in the BY4741 genetic background (Fig. 4 B), indicating that its role in the repair of double strand breaks and other lesions could be important for survival. In agreement with the role of Rev1 in mediating the Sch9-dependent mutagenesis, the deletion of both *SCH9* and *REV1* did not further decrease the age-dependent mutation frequency (Fig. 4 C). In contrast, overexpression of *SCH9*, which models mammalian oncogenic mutations, caused a doubling of the frequency of age-dependent mutations (Fig. 4 E). The deletion of *REV1* reversed the hypermutagenic phenotype of mutants overexpressing *SCH9*, although it also led to early death (Fig. 4, D and E).

REV1 overexpression increased Can^r mutation frequency (Fig. 4 E), and overexpression of *REV1* in *sch9Δ* mutants reversed the protective effect of this longevity mutation only on day 9 and day 11, indicating that *sch9Δ* exerts additional protection independently of Rev1 (Fig. 4 E). Interestingly, larger lesions such as GCRs occurred more frequently in cells lacking *REV1* (10–25-fold higher than in wild-type cells; Fig. 4 G), which suggests that, during aging, the Rev1 protein contributes to the generation of point mutations as part of an emergency response aimed at preventing DNA rearrangements and deletions, which could be lethal.

Polζ consists of a catalytic subunit Rev3 and an accessory Rev7, which associates with Rev1 and is involved mainly in DNA lesion bypass (Gan et al., 2008). To test whether the Polζ was also responsible for an increase in age-dependent mutations, we studied mutants lacking either *REV3* or *REV7*. Cells deficient of Rev3 or Rev7 lived shorter than wild-type cells (Fig. 5, A and C). In both DBY746 and BY4741 genetic backgrounds, Rev3-deficient

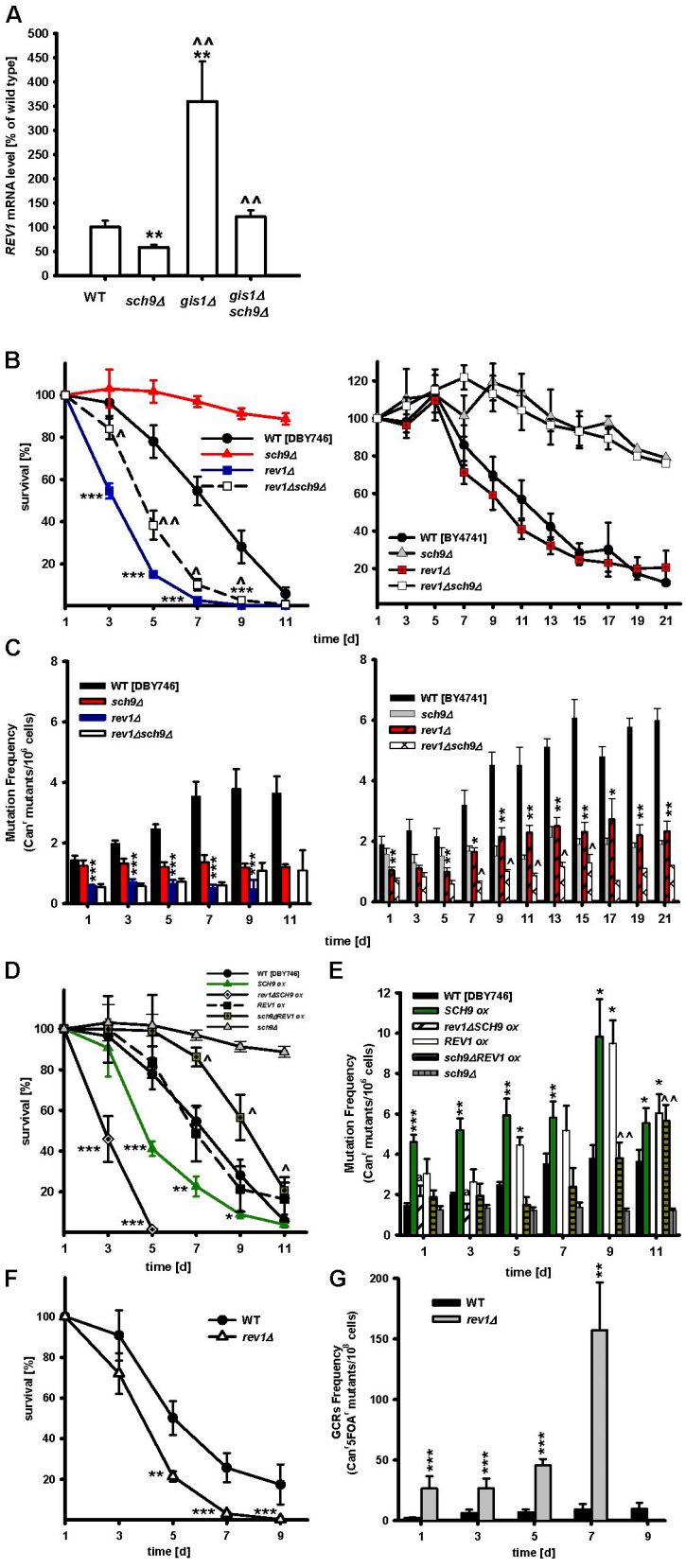

Figure 4. **The age-dependent increase in genomic instability is mediated by Rev1.** (A) mRNA levels of *REV1* in wild-type (WT; DBY746), *sch9*Δ, *gis1*Δ, and *gis1*Δ *sch9*Δ cells. mRNA extracted from 3-d-old cells were subjected to quantitative real-time PCR analysis. **, P < 0.01, mutant versus WT; ^^, P < 0.01, mutant versus *sch9*Δ, *n* = 12, ANOVA test, Tukey's test. (B) Chronological survival and (C) mutation frequency over time in the *CAN1* gene of wild type, *sch9*Δ, *rev1*Δ, and rev1D *sch9*Δ in both the DBY746 and BY4741 genetic backgrounds. ***, P < 0.001; *rev1*Δ versus WT. ^, P < 0.05; *rev1*Δ *sch9*Δ versus *sch9*Δ, two-tailed *t* test at indicated time points (*n* = 9). (D) Chronological survival and (E) mutation frequency over time in the *CAN1* gene of wild-type, *sch9*Δ, *rev1*Δ, and cells overexpressing *SCH9* or *REV1*. *, P < 0.05; **, P < 0.01; ***, P < 0.001; mutant versus WT. ^, P < 0.05; ^^, P < 0.01; *sch9*Δ *REV1ox* versus *sch9*Δ. α, P < 0.05; *rev1*Δ*SCH9ox* versus *SCH9ox*, two-tailed *t* test at indicated time points (*n* = 6–9). (F) Chronological survival and (G) GCRs in the wild type and *rev1*Δ mutants. **, P < 0.01; ***, P < 0.001; *rev1*Δ versus WT, two-tailed *t* test at indicated time points (*n* = 4). Error bars indicate ±SEM.

cells showed a reduction of age-dependent Can^r mutations similar to that observed in the *rev1*Δ mutants (Fig. 5, B and D; and Fig. 4 C). In the BY4741 background, Rev7 deficiency also caused a major reduction in mutation during aging (Fig. 5 B). However, deficiency in Rad30 (Polη), which is mainly involved in the error-free DNA damage bypass (Johnson et al., 1999; Washington et al., 1999; Prakash et al., 2000), caused an elevated age-dependent increase of mutation frequency (Fig. 5 D). These data strongly

Table I. **Mutations spectra observed in Can^r mutant colonies from 7-d-old wild-type, *sch9Δ*, and *rev1Δ* cultures**

Strains	Clone	Type	Base change	Mutations	Position from ATG	Sequence
WT[a]	1	Base substitution	C → T	Proline-leucine	656	5′-TGTTCC**C**TGTC-3′
WT[a]	2	Base substitution	C → T	Proline-serine	937	5′-GCTGCAAAC**C**CC-3′
WT[a]	3	Base substitution	T → G	Asparagine-lysine	1,173	5′-AAA**T**TCAAATA-3′
WT[a]	3	Insertion	G	Frameshift	1,710	5′-GAGGC***G***AATT-3′
WT[a]	4	Base substitution	G → C	Alanine-proline	709	5′-TTTTA**G**CCATTA-3′
WT[a]	4	Deletion	TG	Frameshift	1,098–1,099	5′-TTGCTATTGAGA-3′
WT[a]	5	Base substitution	G → T	Glycine-valine	353	5′-ACGCCG**G**CCCA-3′
WT[a]	5	Insertion	A	Frameshift	1,341	5′-CAAA***A***GTTTTC-3′
WT[a]	6	Deletion	AT	Frameshift	1,129–1,130	5′-GTCACATATCTT-3′
WT[a]	6	Insertion	T	Frameshift (T_3-T_4)	1,086	5′-CCTTT***T***ATTATT-3′
WT[a]	7	Base substitution	G → T	Tryptophan-cysteine	531	5′-GTTTTCTTG**G**CA-3′
WT[a]	7	Deletion	A	Frame-shift (A_3-A_2)	663	5′-AAATATTACGGT-3′
WT[a]	7	Insertion	T	Frameshift (T_3-T_4)	1,086	5′-CCTTT***T***ATTATT-3′
WT[a]	8	Base substitution	G → A	Glutamic A–lysine	679	5′-AATTC**G**AGTTCT-3′
WT[a]	8	Base substitution	G → T	Valine-phenylalanine	907	5′-AACTA**T**TTGGTA-3′
WT[a]	8	Deletion	A	Frameshift	1,217	5′-ATCAAAGAACAC-3′
WT[a]	9	Duplication	NA	248 bp	184–431	NA
WT[a]	10	No PCR	NA	NA	NA	NA
sch9Δ	1	Base substitution	C → A	Serine-STOP	11	5′-AAATT**C**AAAAG-3′
sch9Δ	2	Base substitution	C → A	Serine-STOP	11	5′-AAATT**C**AAAAG-3′
sch9Δ	3	Base substitution	C → A	Serine-STOP	11	5′-AAATT**C**AAAAG-3′
sch9Δ	4	Base substitution	C → A	Serine-STOP	11	5′-AAATT**C**AAAAG-3′
sch9Δ	5	Base substitution	C → A	Serine-STOP	1,244	5′-CTGT**C**AAGGAC-3′
sch9Δ	6	Base substitution	T → C	Phenylalanine-leucine	682	5′-ATTCGAG**T**TCT-3′
sch9Δ	7	Insertion	T	Frameshift (T_6-T_7)	1,386	5′-CTTTTTT**T**GCAT-3′
sch9Δ	8	Base substitution	T → G	Isoleucine-serine	305	5′-GGTACTA**T**TGGT-3′
sch9Δ	8	Insertion	T	Frameshift	1,013	5′-TATTATT***T***CATT-3′
sch9Δ	9	Base substitution	C → A	Serine-STOP	11	5′-AAATT**C**AAAAG-3′
sch9Δ	9	Base substitution	C → A	No change	1,347	5′-TTTT**C**GAATGG-3′
sch9Δ	10	Insertion	T	Frameshift (T_4-T_5)	1,022	5′-GGAC**T**TTTTAGT-3′
sch9Δ	10	Insertion	T	Frameshift (T_6-T_7)	1,386	5′-CTTTTTT**T**GCAT-3′
rev1Δ	1	Base substitution	C → T	Arginine-serine	1,195	5′-GGTTCC**C**GTAT-3′
rev1Δ	2	Insertion	A	Frameshift (A_3-A_4)	702	5′-CAAA***A***GTTTA-3′
rev1Δ	3	Deletion	G	Frameshift	422	5′-GGGTGAAATGG-3′
rev1Δ	3	Deletion	AAA	A_3-A_0	425-427	5′-GGGTGAAATGG-3′
rev1Δ	4	Deletion	G	Frameshift	422	5′-GGGTGAAATGG-3′
rev1Δ	4	Deletion	AAA	A_3-A_0	425-427	5′-GGGTGAAATGG-3′
rev1Δ	5	No PCR	NA	NA	NA	NA
rev1Δ	6	Base substitution	G → A	Tryptophan-STOP	522	5′-GTATTG**G**TTTTC-3′
rev1Δ	7	Base substitution	C → T	Serine-leucine	1,214	5′-TAT**C**AAAGAAC-3′
rev1Δ	8	Base substitution	C → T	Histidine-tyrosine	274	5′-CAAAGA**C**ATATT-3′

Letters in bold indicate base substitutions; bold and italics indicate insertions; underline indicates deletions. NA, not applicable.
[a]from Madia et al. (2008).

suggest that the error-prone Rev1–Polζ complex plays a central role in the generation of point mutations and small insertions/deletions, but prevents GCRs during chronological aging.

To test further the hypothesis that error-prone polymerases mediate age-dependent mutations, we investigated the TLS in 3-d-old wild-type and *sch9Δ* mutant cultures. Nuclear extracts from both wild-type and *sch9Δ* mutant cells were capable of extending the ^{32}P-labeled primer on undamaged DNA templates (Fig. 5 E). In contrast to wild-type cells, nuclear extracts from *sch9Δ* mutants were deficient in lesion bypass activity on the DNA templates containing an abasic site (Fig. 5 E). About 5% TLS efficiency was observed in the wild-type extract when used at 5, 10, or 20 µg, which is in agreement with the lesion bypass efficiency observed in vivo (Pagès et al., 2008). Furthermore, in the nuclear extract from the wild type, ∼20–25% of all extended products represented the incorporation opposite the abasic site, whereas <5% incorporation opposite the lesion was observed in *sch9Δ* (Fig. 5 E).

SCH9 deletion protects against DNA oxidation

The Rev1/Polζ-dependent TLS is activated in response to DNA damage. Thus, we asked whether *SCH9* deficiency might also

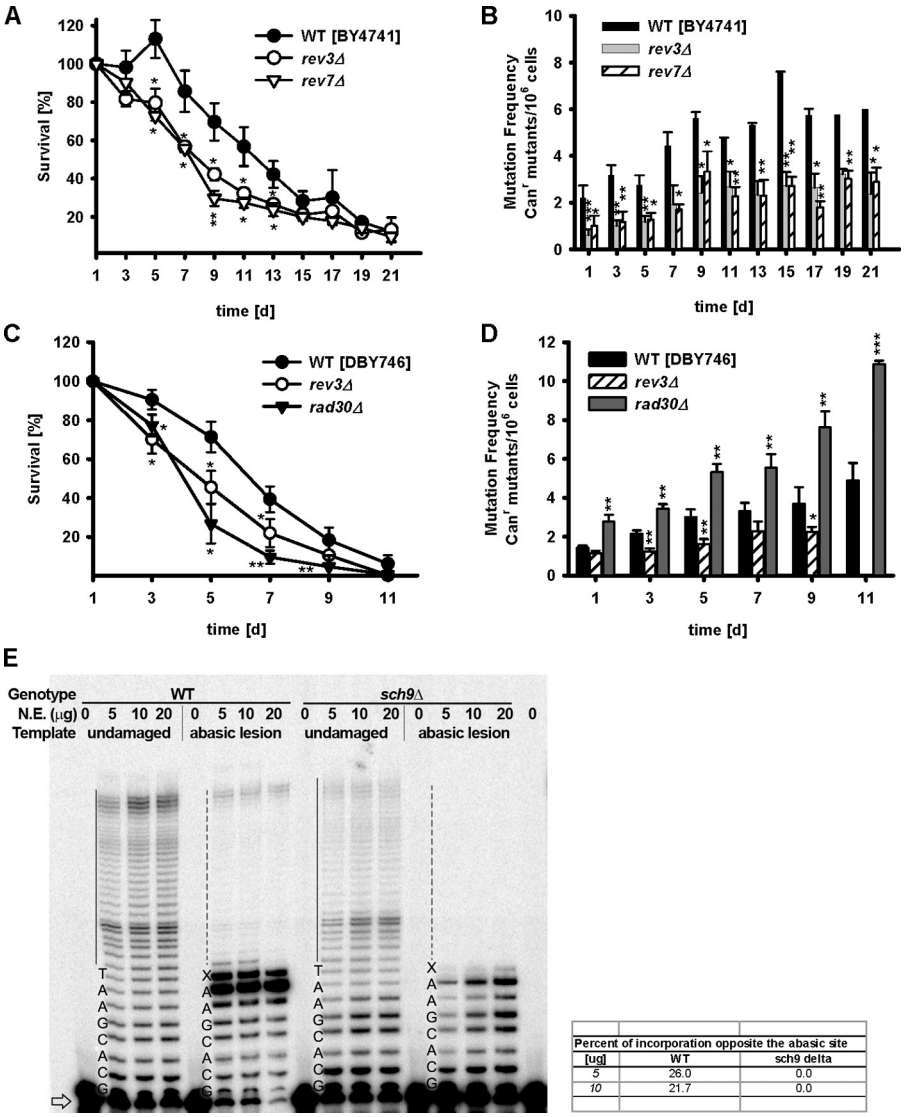

Percent of incorporation opposite the abasic site		
[ug]	WT	sch9 delta
5	26.0	0.0
10	21.7	0.0

Figure 5. **TLS mediates the age-dependent increase in genomic instability.** (A) Chronological survival and (B) mutation frequency (Can^r) of the wild type (BY4741) and mutants deficient of Polζ, *rev3*Δ, and *rev7*Δ. *, P < 0.05; **, P < 0.01; mutants versus wild type (WT) two-tailed *t* test at the indicated time points (*n* = 4). (C) Chronological survival and (D) mutation frequency (Can^r) of the wild type (DBY746), *rev3*Δ, and *rad30*Δ mutants. *, P < 0.05; **, P < 0.01; ***, P < 0.001; mutants versus WT, two-tailed *t* test at the indicated time points (*n* = 6–10). Error bars indicate ±SEM. (E) Abolished TLS in Sch9-deficient cells. Nuclear extracts from 3-d-old stationary phase wild-type (DBY746) and *sch9*Δ mutant cells were incubated with undamaged or abasic site-containing DNA templates for 30 min at 30°C. Primer extension products were analyzed on 19% polyacrylamide gels. There was no lesion bypass observed in *sch9*Δ mutants. Free primers are indicated by the arrow. TLS products are indicated by solid (undamaged) or broken (damaged) lines. On the right, the percentage of incorporation opposite the abasic site is given.

protect against oxidative damage to DNA. Cells were treated with 1 mM H_2O_2 on days 1 and 3, and *Can1* mutation frequency was monitored for 13 d. In the wild-type strain (DBY746), the initial oxidative treatment led to a fourfold increase in Can^r mutations, which continued to increase until day 9, when the great majority of cells were dead (Fig. 6, A and B). In H_2O_2-treated *sch9Δ* cells, mutation frequency and viability, instead, were unaffected or slightly lower, respectively, suggesting that the *SCH9* deletion protects cells against oxidation-induced DNA damage/mutagenesis and cell death (Fig. 6, A and B). Indeed, a sixfold increase of the 8-hydroxy-2′ deoxyguanidine (8-OHdG) level was observed when comparing day 1 versus day 7 in wild-type cells, whereas Sch9-deficient cells showed significantly lower age-dependent accumulation of 8-OHdG (Fig. 6 C). Furthermore, *sch9Δ* mutant cells were protected from oxidative damage (Fig. 6 D), which is in agreement with the lack of Can^r mutation frequency increase during chronological aging (Fig. 6 B). In vivo, 8-OHdG is a prevalent oxidative lesion that, when unrepaired, can lead to G-to-T transversion (Grollman and Moriya, 1993; Moriya, 1993; Le Page et al., 1995). Polζ incorporates A (fives times more likely than C) opposite of 8-OHdG, thus leading to a G → T transversion (Prakash et al., 2005), which is one of the most common mutations found in chronologically aging cells (Table I).

Increased protection against oxidation- but not alkylation-dependent DNA damage in *sch9Δ* mutants

To test whether the lack of *SCH9* decreased age-dependent genomic instability by improving DNA repair, we monitored the mutagenesis induced by either oxidation (hydrogen peroxide [H_2O_2]) or alkylation (methyl methane sulfonate [MMS]) in nondividing cells. Survival, Can^r, and GCRs frequencies in 3-d-old wild-type and *sch9Δ* cells were determined after exposure to 100 mM H_2O_2 for 30 min or to 0.02% of MMS for 50 min. After treatment, cells were washed four times and allowed to repair DNA without dividing in toxin-free expired synthetic dextrose complete (SDC) medium obtained from parallel aging cultures. Can^r mutations and GCRs were measured 30 min, 2 h, and 5 h after the end of each treatment. The exposure to hydrogen peroxide had little or no effect on *sch9Δ* viability (10% cell death), but

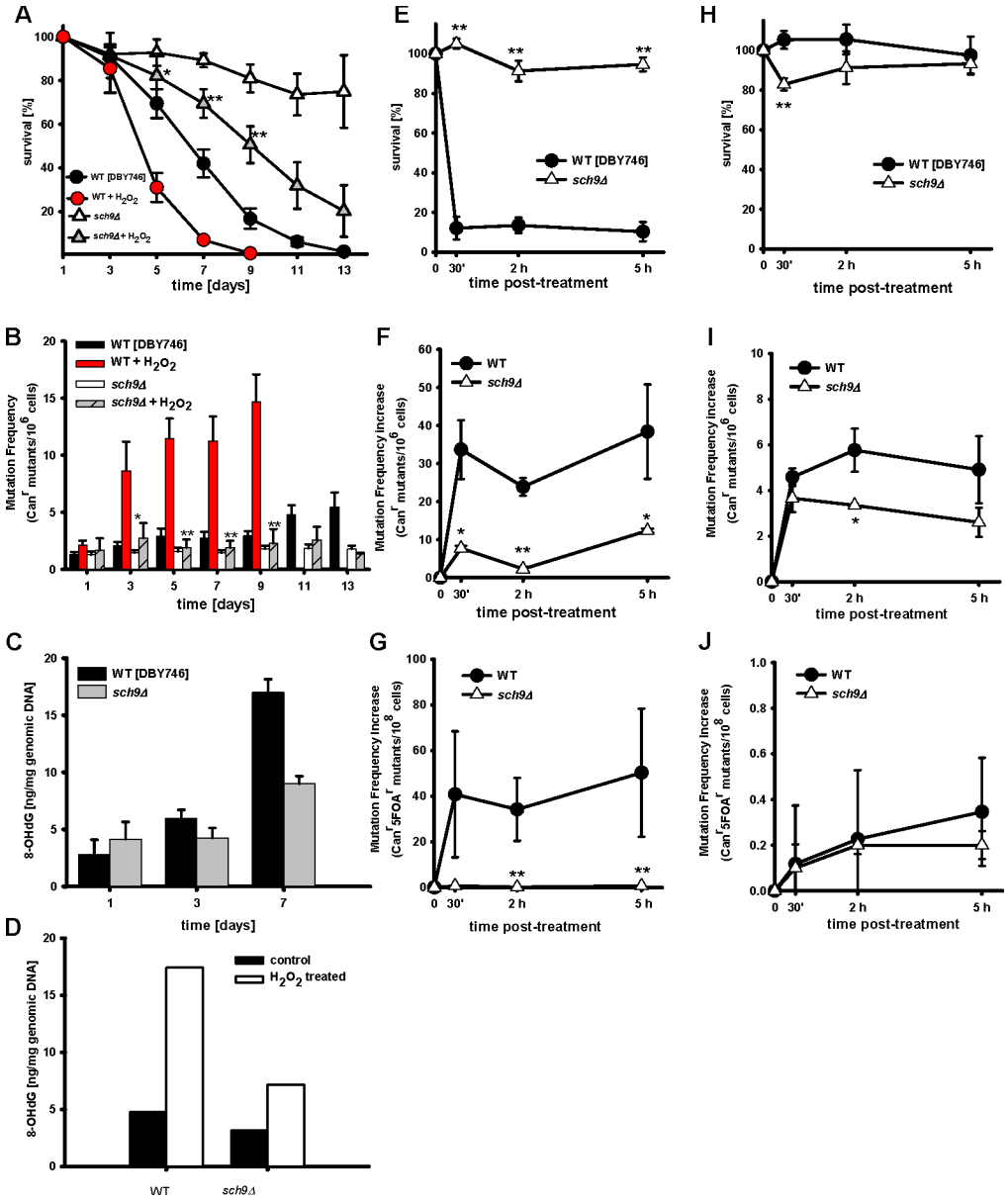

Figure 6. **The lack of *SCH9* protects against oxidative stress-induced genomic instability.** (A) Chronological survival and (B) mutation frequency (Can^r) of the wild type (DBY476) and *sch9*Δ mutants. Cells were treated with 1 mM H_2O_2 at day 1 and day 3. *, $P < 0.05$; **, $P < 0.01$; *sch9*Δ versus wild type (WT), two-tailed *t* test at the indicated time points ($n = 4$). (C) 8-OHdG contents in the wild type (DBY746) and *sch9*Δ mutants during chronological aging. (D) Day 3 SDC wild-type and *sch9*Δ cultures were treated with 1 mM H_2O_2 for 48 h.The mean of two independent experiments in duplicate is presented. (E–G) Wild-type (DBY746) and *sch9*Δ mutant cells were exposed to 100 mM H_2O_2 for 30 min. Survival (E), mutation frequency (F; Can^r), and GCR (G; Can^{r}5FOA^r) were monitored at 30 min, 2 h, and 5 h after the end of H_2O_2 treatment. (H–J) Wild-type (DBY746) and *sch9*Δ mutant cells were exposed to 0.02% MMS for 50 min. Error bars indicate ±SEM. Survival (H), mutation frequency (I; Can^r), and GCR (J; Can^{r}5FOA^r) were monitored at 30 min and 5 h after the end of MMS treatment. For E–J, data represent mean ± SEM (error bars), $n = 3$. *, $P < 0.05$; **, $P < 0.01$; two-tailed *t* test at the indicated time points, *sch9*Δ versus WT.

killed 90% of the wild-type cells (Fig. 6 E). 2 h after treatment with H_2O_2, Can^r mutation frequency in *sch9Δ* showed only a minor increase and remained sixfold lower than that of wild-type cells (Fig. 6 F). Similarly, the *sch9Δ* mutant did not show any increase in GCRs frequency in contrast to the wild type, which displayed a >100-fold increase in GCRs by 5 h (Fig. 6 G).

In contrast to its role in protecting against oxidative stress-induced mutations, the *sch9Δ* mutation did not protect against alkylation-induced DNA damage (Fig. 6, H, I and J). Wild-type cells were slightly more sensitive to 0.02% MMS, and *sch9Δ* only gave a small amount of protection against mutations and GCRs in response to MMS (Fig. 6, I and J). These results indicate that *sch9Δ* mutant cells are not well protected from alkylating DNA damage but are partially protected from alkylation-induced point mutations and small insertions/deletions (Fig. 6 I).

The role of superoxide in age-dependent mutations

Based on the age-dependent increase of 8-OHdG levels (Fig. 6 C), the spectra of Can^r mutations (Table I), the involvement of the

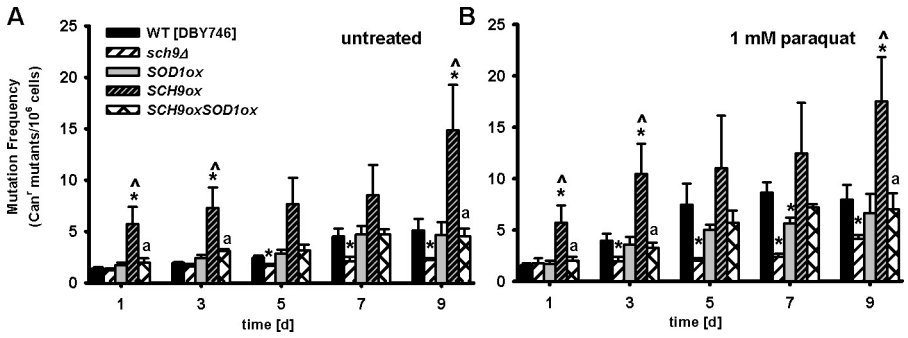

Figure 7. ***SOD1* overexpression attenuates age-dependent oxidative stress and *SCH9* overexpression–induced genomic instability.** (A) Mutation frequency (Can^r) of cells during normal chronological aging. (B) Mutation frequency (Can^r) of cells treated with 1 mM paraquat on day 1 and on day 3. Strains shown are wild type (WT; DBY476), *sch9*Δ, and cell overexpression of *SOD1* and/or *SCH9*. *, $P < 0.05$; mutant versus WT. ^, $P < 0.01$; mutant versus *sch9*Δ, two-tailed *t* test at the indicated time points ($n = 5$). Error bars indicate ±SEM.

Rev1–Polζ complex in age-related mutagenesis (Figs. 4 and 5), and the protection against oxidative damage to DNA exerted by deficiency in *SCH9* (Fig. 6), we studied the role of superoxide and oxidative DNA damage in Sch9- and age-dependent genomic instability.

The life span extension associated with deficiencies in Sch9 and Ras2/cAMP/PKA requires the expression of the mitochondrial superoxide dismutase (MnSOD; Fabrizio et al., 2003) and of the stress response transcription factors Msn2/4 and Gis1 (Pedruzzi et al., 2000; Wei et al., 2008). Both the stress response element (STRE) and post-diauxic shift motif (PDS) are present in the promoter region of *SOD2*, which is up-regulated in cells lacking Sch9 (Fig. S2 A). The genome-wide expression profiling also indicated that deletion of *SCH9* causes a metabolic switch from the TCA cycle and respiration to glycolysis and glycerol biosynthesis, as well as a general reduction of mRNA levels of proteins targeted to mitochondria (Wei et al., 2009), which is in agreement with the reduced generation and/or level of superoxide in *sch9Δ* mutants.

Overexpression of the cytosolic Cu, Zn superoxide dismutase *SOD1* (introduction of plasmid YEp352-*SOD1ox*[URA3] induced an eightfold increase of *SOD1* mRNA level compared with the wild type; Figs. S2 B and S3), was able to completely abolish the detrimental effect of the overexpression of *SCH9* on either age-dependent spontaneous or paraquat-induced genomic instability (Fig. 7, A and B). Moreover, the overexpression of either *SOD1* or *SOD2* (introduction of plasmid YEp351-*SOD2ox*[LEU2] induced a fourfold increase of the *SOD2* mRNA level compared with the wild type; Figs. S2 B and S3) was effective in attenuating age-dependent mutation frequency increase in Gis1-deficient cells and down-regulating the *REV1* mRNA level (Fig. 8, A–C). To test whether the combination of both a high superoxide and *REV1* level contribute to age-dependent mutations, we treated *rev1Δ* mutants and *REV1* overexpressors with 1 mM paraquat (Fig. 9, A–C). *REV1* overexpression did not increase further paraquat-dependent mutagenesis, possibly because the superoxide generated by paraquat might have maximized *REV1* expression (Fig. 9 C). *SOD1* and *SOD2* overexpression did cause a significant decrease in the *REV1* mRNA level (Fig. 9 D). These results indicate that the Sch9-dependent accumulation of oxidative DNA damage is the major source of age-dependent genomic instability in nondividing cells. We propose that during the first round of replication, the Rev1–Polζ complex processes the oxidation-induced abasic sites and generates base substitutions to avoid GCRs and possibly cell death (Fig. 9 E).

Discussion

Age-dependent DNA damage and cancer are widely believed to depend on mutations associated with the number of divisions completed by a cell. Here, in the study of a unicellular eukaryote, the frequencies of Can^r mutations and GCRs (Fig.1 B and D) reached 3- and 20-fold, respectively, higher levels in cells aging under nondividing conditions than in the population resulting from the many divisions necessary for the expansion from the initial 100 thousand to 1 billion cells contained in each aging study (we refer to the Can^r and GCRs frequencies reached in the cell population at the end of the growth phase on day 1).

Mutated Ras, Akt, and PTEN are widely believed to contribute to cancer by promoting growth and preventing apoptosis (Pollak et al., 2004). Based on mammalian studies, inhibition of Ras and Akt is predicted to slow down growth and promote the apoptosis of cancer cells. Studies by our laboratory and others have shown that yeast homologues of mammalian Ras and Akt/S6K promote aging, oxidative stress, and age-dependent mutations (Fabrizio et al., 2001, 2003, 2004; Hlavatá and Nyström, 2003). Although Sch9 and Ras promote growth in *S. cerevisiae*, we show that Sch9 can promote DNA damage during aging in nondividing cells. Interestingly, the separation of aging wild-type cultures by a density gradient revealed that quiescent cells, otherwise considered stable and protected, exhibit an elevated DNA mutation frequency compared with nonquiescent cells (Fig. 2 E). Our data suggest that DNA damage and mutations including GCRs occur mostly in old cells and are associated with a shorter life span, but do not provide conclusive evidence for the role of DNA damage as a major factor in the aging process (Vijg, 2008). Sch9 appears to be responsible for the major portion of age-dependent increase in DNA mutations because cells lacking *SCH9* displayed reduced point mutations, small insertions/deletions, and GCRs, whereas cells overexpressing *SCH9*, which models mammalian Akt-activating oncogene mutations (PTEN etc), displayed a significant increase in mutations. The effect of Sch9 on age-dependent mutations did not appear to be simply due to its effect on survival because, at a comparable percent of survival, the cumulative frequency of mutations in *sch9Δ* was less than half of that in wild-type cells (Fig. 1 C).

We observed a higher occurrence of multiple mutations within a short stretch of DNA in Can^r mutants from 7-d-old wild-type cultures than in *sch9Δ* mutants (Table I). This mutation profile was reminiscent of that caused by the error-prone PolIV and PolV polymerases, which are involved in increased

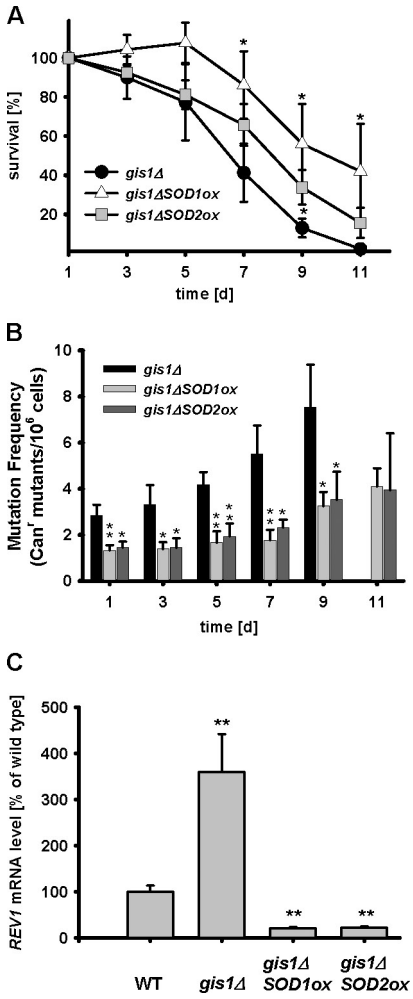

Figure 8. **Oxidative stress and genomic instability.** (A and B) Overexpression of *SOD1* or *SOD2* extends life span and reduces genomic stability associated with *gis1*Δ mutants. *, P < 0.05; **, P < 0.01; compared with *gis1*Δ, two-tailed *t* test at the indicated time points ($n = 4$). (C) mRNA levels of *REV1* in wild-type (WT; DBY746), *gis1*Δ, and *gis1*Δ cells overexpressing either *SOD1* or *SOD2*. mRNA extracted from 3-d-old cells was subjected to quantitative real-time PCR analysis. **, P < 0.01; mutant versus WT ($n = 12$, ANOVA test, Tukey's test). Error bars indicate ±SEM.

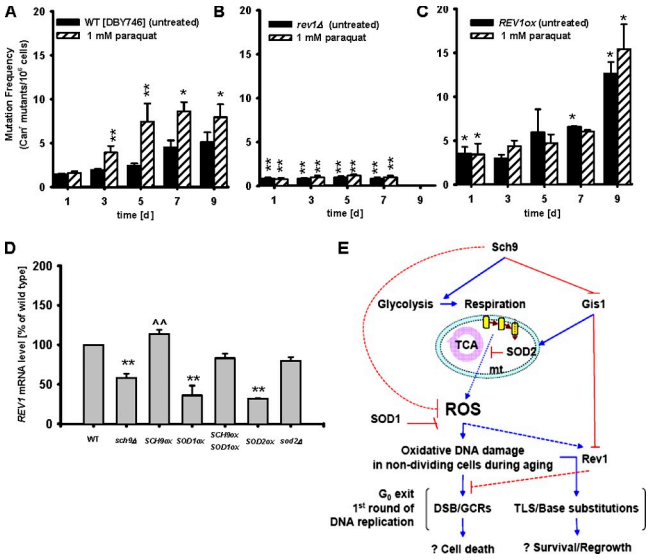

Figure 9. **Rev1 mediates oxidative stress induced genomic instability.** (A–C) Mutation frequency (Can^r) of the wild type (DBY476), *rev1*Δ, and cells overexpressing *REV1* (*REV1*ox) during chronological aging and under oxidative stress (1 mM paraquat at day 1 and at day 3). *, P < 0.05; **, P < 0.01; *rev1*Δ versus wild-type (WT) untreated, two-tailed *t* test at the indicated time points ($n = 4$). Error bars indicate ±SEM. (D) *REV1* mRNA levels at day 3. *REV1* mRNA level were normalized to *ACT1* and represent mean ± SEM (error bars) of the percentage of wild type. **, P < 0.01; compared with WT. ^^, P < 0.01; compared with *sch9*Δ (two-tailed *t* test, $n = 8–12$). (E) Modulation of oxidative stress and genomic instability by Sch9. During chronological aging, the oncogene homologue *SCH9* inhibits the expression of genes involved in glycolysis and promotes respiration. Sch9 also regulates the error-prone Polζ complex component Rev1 through the stress response transcription factor Gis1. Accumulation of oxidative DNA damage during aging activates Rev1-mediated TLS, which leads to increased base substitutions and reduced GCRs in the first round of DNA replication when cells exit the arrested state.

mutability in nondividing *E. coli* (McKenzie et al., 2001; Kobayashi et al., 2002), and of that caused by eukaryotic TLS polymerases (Rev1, Polζ, and Rad30; Waters et al., 2009). In the *sch9Δ* mutants, base substitutions were mostly C → A, followed in one case only by a T insertion (Table I), suggesting that the lack of *SCH9* not only reduced the frequency of spontaneous age-dependent mutations but also prevented multiple mutations within a short stretch of DNA sequence.

REV1 was among the most down-regulated DNA repair-related genes in the *sch9Δ* mutant, and its expression (mRNA level) was reduced 40% compared with the wild type on day 3 (Figs. 3 C and 4 A). The lack of *REV1* prevented the mutation frequency increase associated with aging or induced by *SCH9* overexpression, but did not affect the mutation frequency of *sch9Δ* (Fig. 4). Rev1 expression is threefold higher during G2/M than in G1 phase (Waters and Walker, 2006; Sabbioneda et al., 2007). Based on these results and on our FACS data (Fig. S1 A), we would have expected a smaller reduction of the *REV1* mRNA level than the 60% measured in Sch9-deficient cells if its regulation was only dependent on the cell cycle. These results indicate additional regulation/activation of *REV1* expression in aging cells.

rev1Δ mutants showed an 80% decrease in mutation frequency compared with wild-type cells (Fig. 4 C). Rev1 is known to insert C opposite the abasic site (Nelson et al., 1996), but it has also been shown to insert all four nucleotides to repair a gap (Haracska et al., 2002). This mutagenic role of Rev1 has been confirmed in vivo (Auerbach et al., 2005). The base substitutions observed in the *CAN1* gene (Table I) were consistent with the deoxycytidine monophosphate transferase activity of Rev1 or its modulation of thymidine monophosphate insertions opposite an abasic site, although part of them are likely to be generated independently of TLS. Furthermore, Rev1 can play a structural role in aiding polymerases bypass lesion sites, which does not depend on its nucleotidyl transferase activity (Nelson et al., 2000; Lawrence, 2004). In this case, the insertion of the nucleotide opposite an abasic site is catalyzed by polymerase δ (Haracska et al., 2001).

The deletion of *REV1* in wild-type cells blocked the generation of multiple mutations/insertions/deletions within a short stretch of DNA sequence (Table I). Previous studies from the laboratories of S. Jinks-Robertson and T.A. Kunkel (Kozmin et al., 2003; Minesinger et al., 2006) described spontaneous "complex"

mutational events, in which a frameshift is accompanied by one or more base substitutions. These events depended on the mutagenic TLS polymerase Polζ activity, which functions in association with Rev1 (Minesinger et al., 2006). Our results show that age-dependent mutagenesis was reduced in cells lacking either *REV3* or *REV7*, the two subunits of Polζ polymerase, but was increased in mutants lacking *RAD30*, which is regarded as an error-free DNA damage bypass enzyme (Johnson et al., 1999; Washington et al., 1999; Prakash et al., 2000).

These findings support the hypothesis that the majority of age-dependent mutations are generated through the activity of the Rev1–Polζ error-prone complex, whose activity may be elevated in aging cells (Fig. 5 E). The down-regulation of Rev1 expression alone, however, may not explain the complete absence of TLS activity in *sch9Δ* mutants. Rev1 is not absolutely required for TLS in yeast (Pagès et al., 2008); we cannot exclude the possibility that the deficiency and/or modification in other important TLS components, such as proliferating cell nuclear antigen ubiquitination and/or Polζ itself, contributed to the complete absence of TLS in *sch9Δ* mutant cells (Fig. 5 E).

Mutants lacking *SCH9* were highly protected against exogenous oxidative stress (Fabrizio et al., 2001). This study shows that the deficiency in *SCH9* protected against endogenous age-dependent oxidative damage to DNA, as indicated by the level of 8-OHdG (Fig. 6 C). The elevated expression of *SOD2* and protection of the DNA against oxidative damage in *sch9Δ* mutants, together with the effect of the overexpression of both *SOD1* and *SOD2* in reducing point mutations, indicate that Sch9 promotes mutations by a superoxide-dependent mechanism. We propose that superoxide and the oxidized DNA cause an increased expression of *REV1* and activation of the error-prone Polζ, which result in point mutations during the first round of replication in order to prevent double strand breaks and GCRs (Fig. 9 E).

Although the deletion of *SCH9* causes Gis1-dependent repression of *REV1* expression (Fig. 4 A), Sch9 and Gis1 may not necessarily function in the same pathway as Rev1/Polζ. The superoxide production and DNA oxidation regulated by Sch9 may instead directly lead to the activation of the error-prone system (Brunet et al., 2004; Shen et al., 2007). In fact, the overexpression of either *SOD1* or *SOD2* was sufficient to decrease *REV1* expression (Fig. 9 D).

Recent work in neurons and mice suggests that somatic mutations associated with Huntington's disease occur during the removal of oxidation lesions by an error-prone mechanism dependent on the base excision repair enzyme Ogg1 (Kovtun et al., 2007). Our data raise the possibility that down-regulation of the mammalian Akt/S6K signaling pathway implicated in life span regulation may also regulate oxidative damage as well as error-prone polymerases that can cause DNA damage and diseases during aging. Notably, down-regulation of Rev1 in human cells reduced UV-dependent mutations (Gibbs et al., 2000), which suggests that the role of this protein is at least partially conserved from yeast to humans. The connection between oncogene homologs, Rev1, and age-dependent genomic instability observed in the simple *S. cerevisiae* model has not been demonstrated in mammals. However, the recent papers showing reduced age-dependent cancer incidence in mice deficient in IGF-I (Vergara et al., 2004) or Akt (Skeen et al., 2006), and the reduction in tumors in *C. elegans* deficient in the IGF-I–like receptor DAF-2 (Pinkston et al., 2006) are consistent with our previous and present results indicating a link between these oncogenes, mutagenesis, and cancer (Longo et al., 2008). It will be important to determine whether these conserved antiaging pathways may regulate, in addition to cell growth and apoptosis, oxidation damage of DNA and error-prone DNA repair proteins in both dividing and nondividing cells.

Materials and methods

Yeast strains

The experiments were performed in DBY746 (*MATα,leu2-3,112,his3Δ1,trp1-289,ura3-52,GAL⁺*), provided by D. Botstein, Massachusetts Institute of Technology, Cambridge, MA. The strain BY4741 (*MATa,his3Δ1leu2Δ0, met15Δ0,ura3Δ0*; Thermo Fisher Scientific) was used to confirm the results obtained with the DBY746 strain.

Strain EH150 (*MATa,lys2ΔBglII,trp1-Δ,his3-Δ200,ura3-52,ade2-1o*) was used for the small insertion/deletion mutation assay (provided by E. Heidenreich, Institute of Cancer Research, Medical University of Vienna, Vienna, Austria). The *sch9Δ* mutant has been described previously (Fabrizio et al., 2001). All the mutant strains were originated in the different backgrounds by one-step gene replacement according to Brachmann et al. (1998). K.A. Morano (University of Texas Medical School, Houston, TX) provided low copy plasmid pRS416-HA3-*SCH9*. Multicopy 2 μ plasmid carrying *REV1* was obtained from Thermo Fisher Scientific. Overexpressor plasmids for *SOD2* and *SOD1* were constructed in multicopy vectors (YEp352 and YEp351, respectively) and have been described previously (Fabrizio et al., 2003).

Growth conditions

Yeast chronological life span was monitored in expired SDC medium by measuring colony-forming units (CFUs) every 48 h. The number of CFUs at day 1 was considered to be the initial survival (100%) and was used to determine the age-dependent mortality (Fabrizio and Longo, 2003).

Can1 mutation frequency measurements

Spontaneous mutation frequency was evaluated by measuring the frequency of mutations of the *CAN1* (*YEL063*) gene. In brief, overnight inoculations were diluted in liquid SDC medium and incubated at 30°C. The cells' viability was measured every 2 d starting at day 1 by plating appropriate dilutions onto yeast extract peptone dextrose (YPD) medium plates and counting the CFUs. To identify the canavanine-resistant mutants (Can^r) in the liquid culture, an appropriate number of cells (starting amount of 2×10^7 cells) was harvested by centrifugation, washed once with sterile water, and plated on selective medium (SDC-Arg supplemented with 60 μg/ml L-canavanine sulfate). Mutant colonies were counted after 3–4 d. The mutation frequency was expressed as the ratio of Can^r to total viable cells.

Large-scale measurement of GCRs

To detect GCRs, a DBY476 background strain was generated by the replacement of *HXT13* (*YEL069*), encoding for a highly redundant hexose transporter, with a *URA3* cassette (Chen and Kolodner, 1999). *HXT13* is located 7.5 kb telomeric to *CAN1* on chromosome V. The experiment was conducted similarly to that described for the *Can1* mutations, but the detection for the loss of both *CAN1* and *URA3* was performed on SDC-Arg plates containing 1 mg/ml 5-fluoroorotic acid (5FOA) and 60 μg/ml L-canavanine. Mutant colonies were counted after 3–4 d.

Measurement of age-dependent small insertion/deletion mutations

Based on the experimental design proposed by Heidenreich et al., (2003) and Heidenreich and Wintersberger (1998), we generated *sch9Δ* mutants in a Lys$^-$ strain (EH150) in which a lys2ΔBglII mutation was constructed by filling in a BglII restriction site of the *LYS2* gene. The resulting +4 shift in the open reading frame causes an auxotrophy for lysine that can be reversed by small age-dependent insertion/deletion mutations. Cells were plated onto selective SDC-Lys medium. The experiments were performed similarly to the one described for the *Can1* mutations.

Measurement of age-dependent single-base substitution mutations

To monitor the frequency of reversion of a base substitution, we used the strain DBY746 that carries a *trp 1–289* amber mutation (C → T at residue

403 of the coding sequence) and measured the frequency of *trp1-289* to Trp^+ reversions (Capizzi and Jameson, 1973). Cells were plated onto selective SDC-Trp medium. The experiments were performed similarly to the one described for the *Can1* mutations.

Isolation of quiescent and nonquiescent cells

Percoll density gradient (GE Healthcare) was prepared using the protocol described by Allen et al., (2006). Straight after the separation, cells were plated on YPD and on SDC-Arg medium supplemented with 60 µg/ml L-canavanine sulfate solid media to measure viability (CFUs) and determine mutation frequency, respectively (Madia et al., 2008). Morphological characterization was performed with a microscope (DM IRB; Leica) equipped for phase contrast and fluorescence light microscopy. Cells were stained either with 0.1 mg/ml phloxin B (Sigma-Aldrich) or 25 µM Calcofluor White N2R fluorescent brightener 28 (Invitrogen). Lower- and upper-fraction cells were also examined microscopically, without previous sonication, for the presence of new buds.

FACS analysis and budding index

Cells from exponentially proliferating cultures of wild-type and *sch9Δ* strains were inoculated into SDC medium at an initial density of 5×10^5/ml, and continuously cultured for 7 d at 30°C with rotary shaking. Aliquots of cells removed from each culture at the indicated times were collected to measure budding index and to measure DNA content by flow cytometry, as described previously (Madia et al., 2008). Data were calculated by MODFIT (Verity Software House).

8-OHdG measurement

8-OHdG content was estimated by an ELISA assay, using a *8-OHdG Check* kit (Cosmo Bio Co., Ltd). Nuclear DNA was isolated from wild-type and *sch9Δ* mutant cells by mechanical release of DNA from cells disrupted with glass beads. About 50×10^8 cells were washed off the medium and suspended in 4 ml of lysis buffer (Tris-EDTA buffer, 1% SDS, 2% Triton X-100, and 100 mM NaCl). DNA was extracted using the standard phenol/chloroform method and finally suspended in Tris-EDTA buffer. 200 µg of DNA were digested with nuclease P_1 and alkaline phosphatase prior to the ELISA assay, according to the manufacture's instructions.

***CAN1* sequencing**

Canavanine-resistant clones from wild-type (DBY746) and *sch9Δ* strains were collected during a chronological life span study. Genomic DNA was isolated using standard glass beads/chloroform-phenol procedure. Two primer sets were used for PCR amplification to cover the *CAN1/YEL063C* open reading frame. PCR products were gel purified and sequenced using the amplification primers (both directions). Additional primers were used to confirm the sequencing results when necessary (Madia et al., 2008). All primers were synthesized by Integrated DNA Technologies, Inc.; sequencing was performed by Laragen, Inc. Identification of mutation was performed using Mutation Surveyor version 3.00 (Softgenetics, LLC).

Microarray gene expression analysis

Day 2.5 wild-type and *sch9Δ* cultures were used to extract total RNA according to the acid phenol method. Total RNA from three independent cultures of each strain was used as a template to synthesize complementary RNA (cRNA). cRNA was hybridized to GeneChip Yeast Genome 2.0 array (Affymetrix). For each wild-type sample, three replicates of a mutant were normalized with respect to the wild-type reference array. Then, the four arrays were summarized by the median polishing method in robust multi-array average (RMA). This leads to three estimates of expression fold changes of the mutant versus the wild type. In total, we had nine estimates of expression fold changes from three wild-type references, and the median was taken as the final estimate (Cheng et al., 2007a,b). The change in expression level between a baseline and an experimental array is included in Table S2.

Quantification of mRNA by real-time PCR

Total RNA was extracted with a standard phenol/chloroform method. First-strand cDNA was synthesized using SuperScript II reverse transcription (Invitrogen) and random primers. Real-time PCR was performed using the BIO-RAD Opticon 2 detection system in the presence of SYBR-green I dye (Bio-Rad laboratory). The forward and reverse primers for *REV1* were 5′-GCGAAAAGGATAGTCGCTTG-3′ and 5′-CTTCCATGCGGAGAGA-TGAT-3′, respectively. The forward and reverse primers for *SOD1* were 5′-TTTGATCAAGCTTATCGGTCCT-3′ and 5′-TTGGTTAGACCAATGACAC-CAC-3′, respectively. The forward and reverse primers for *SOD2* were 5′-CTACAACCAGGATACCGTCACA-3′ and 5′-CTTCTGGATGCTTCT-TTCCAGT-3′, respectively. The forward and reverse primers for the housekeeping gene *ACT1* were 5′-AGCTCCAATGAACCCTAAATCA-3′ and 5′-ACGACGTGAGTAACACCATCAC-3′, respectively. The concentration (ng/µl) of both genes was calculated by reference to the respective standard curve. Relative gene expression was expressed as a ratio of *REV1* gene concentration to *ACT1* concentration, and the values given represent the percentage of wild type of the mean gene expression ± SEM.

TLS in yeast cell-free nuclear extracts

Yeast cell-free nuclear extracts were prepared according to the established protocol (Wang, 2006). In brief, yeast cells from indicated strains (wild type or *sch9Δ*) were grown at 30°C in SDC medium until day 3. Cells were harvested by centrifugation for 10 min, washed in water, and suspended at 0.1 g/ml in 0.1M EDTA, pH 8.0/10 mM dithiothreitol buffer. After a 30-min incubation, cells were pelleted and suspended at 1 g/ml in 1 M sorbitol solution, and yeast lytic enzyme (Zymo Research Corporation) was added at 1.4–2.8 mg/g of cells. Spheroplasts were resuspended in Ficoll buffer and lysed with a Teflon glass homogenizer. Nuclei were recovered from the supernatant by at least four consecutive centrifugations and resuspended in lysis buffer. After precipitation with ammonium sulfate, proteins were dialyzed in Hepes buffer. Precipitates formed during dialysis were removed by centrifugation, and the resulting nuclear extracts were stored at −70°C. Extract concentration was quantified using a Pierce BCA protein assay (Thermo Fisher Scientific).

48-mer undamaged or damaged oligonucleotide substrate (48 mer) 5′-TCGATACTGGTACTAATGATTAACGACTXAAGCACGTCCGTACCA-TCG-3′ (X is either T for the undamaged or tetrahydrofurane-type of abasic site for the damaged template) and a 12-mer primer 5′-CGATGGTACGGA-3′ were synthesized on a 3400 DNA Synthesizer (Applied Biosystems) and purified by denaturing PAGE. TLS reactions (50 µl volume) were performed in a TLS buffer (20 mM Hepes, pH 7.8, 7 mM $MgCl_2$, 1 mM DTT, and 25 mM NaCl) containing 200 µM deoxynucleotide triphosphate, 100 nM of ^{32}P-labeled primer annealed to the template (undamaged or damaged), and the indicated amount of wild-type or *sch9Δ* nuclear extract (0, 5, 10, or 20 µg). After incubation at 30°C for 30 min, reactions were terminated by addition of 10 mM EDTA and 0.4 mg/ml proteinase K, and incubated for an additional 30 min at 37°C. TLS reaction products were purified by extracting twice with phenol:chloroform:isoamyl alcohol, separated on a 19% denaturing PAGE. Gel band intensities were measured by phosphorimaging with ImageQuant software (GE Healthcare).

Statistical analysis

Longevity curves and mutation frequency curves were analyzed by an unpaired two-tailed *t* test (P-values were $P < 0.001$, $P < 0.01$, and $P < 0.05$) on the data for each pair of strains at each day. RT-PCR data were analyzed by a one-way analysis of variance (ANOVA) test.

Online supplemental material

Fig. S1 shows the percentage distribution in each cell cycle compartment, as resulted from the FACS analysis from wild-type and *SCH9*-deficient cultures at early time points, and the cell cycle profiles of quiescent and nonquiescent fractions from wild-type and *SCH9*-deficient cultures after density gradient separation. Fig. S2 shows the mRNA *SOD*s and *REV1* levels in 3-d-old wild-type, *sch9Δ*, *gis1Δ*, and *gis1Δsch9Δ* mutants and in cells overexpressing *SCH9* and mRNA *SOD*s and *REV1* levels in 3-d-old wild-type and *sch9Δ* mutants cells treated with 1 mM paraquat for 48 h. Fig. S3 shows the survival and age-dependent mutation frequency of plasmid vectors. Table S1 shows the percentage of early regrowth in wild-type and Sch9-deficient cells. Table S2 shows the microarray gene expression analysis of DNA repair genes in *sch9Δ* cells. Online supplemental material is available at http://www.jcb.org/cgi/content/full/jcb.200906011/DC1.

We thank Dr. E. Heidenreich for providing strain EH150 and Dr. Kevin A. Morano for providing the SCH9 overexpressing plasmid. We thank Dr. Michael Lieber for very helpful comments and Drs. William C. Burhans and Martin Weinberger for their assistance in FACS analysis.

This work was supported in part by an American Federation for Aging Research grant and by National Institutes of Health grants AG20642, AG025135, and GM075308.

Submitted: 2 June 2009
Accepted: 16 July 2009

References

Allen, C., S. Büttner, A.D. Aragon, J.A. Thomas, O. Meirelles, J.E. Jaetao, D. Benn, S.W. Ruby, M. Veenhuis, F. Madeo, and M. Werner-Washburne.

2006. Isolation of quiescent and nonquiescent cells from yeast stationary-phase cultures. *J. Cell Biol.* 174:89–100.

Anisimov, V.N., L.M. Berstein, I.G. Popovich, M.A. Zabezhinski, P.A. Egormin, M.L. Tyndyk, I.V. Anikin, A.V. Semenchenko, and A.I. Yashin. 2005. Central and peripheral effects of insulin/IGF-1 signaling in aging and cancer: antidiabetic drugs as geroprotectors and anticarcinogens. *Ann. N. Y. Acad. Sci.* 1057:220–234.

Aragon, A.D., A.L. Rodriguez, O. Meirelles, S. Roy, G.S. Davidson, P.H. Tapia, C. Allen, R. Joe, D. Benn, and M. Werner-Washburne. 2008. Characterization of differentiated quiescent and nonquiescent cells in yeast stationary-phase cultures. *Mol. Biol. Cell.* 19:1271–1280.

Auerbach, P., R.A. Bennett, E.A. Bailey, H.E. Krokan, and B. Demple. 2005. Mutagenic specificity of endogenously generated abasic sites in *Saccharomyces cerevisiae* chromosomal DNA. *Proc. Natl. Acad. Sci. USA.* 102:17711–17716.

Bartkova, J., Z. Horejsí, K. Koed, A. Krämer, F. Tort, K. Zieger, P. Guldberg, M. Sehested, J.M. Nesland, C. Lukas, et al. 2005. DNA damage response as a candidate anti-cancer barrier in early human tumorigenesis. *Nature.* 434:864–870.

Brachmann, C.B., A. Davies, G.J. Cost, E. Caputo, J. Li, P. Hieter, and J.D. Boeke. 1998. Designer deletion strains derived from *Saccharomyces cerevisiae* S288C: a useful set of strains and plasmids for PCR-mediated gene disruption and other applications. *Yeast.* 14:115–132.

Brunet, A., L.B. Sweeney, J.F. Sturgill, K.F. Chua, P.L. Greer, Y. Lin, H. Tran, S.E. Ross, R. Mostoslavsky, H.Y. Cohen, et al. 2004. Stress-dependent regulation of FOXO transcription factors by the SIRT1 deacetylase. *Science.* 303:2011–2015.

Burhans, W.C., and M. Weinberger. 2007. DNA replication stress, genome instability and aging. *Nucleic Acids Res.* 35:7545–7556.

Campisi, J. 2001. From cells to organisms: can we learn about aging from cells in culture? *Exp. Gerontol.* 36:607–618.

Capizzi, R.L., and J.W. Jameson. 1973. A table for the estimation of the spontaneous mutation rate of cells in culture. *Mutat. Res.* 17:147–148.

Chen, C., and R.D. Kolodner. 1999. Gross chromosomal rearrangements in *Saccharomyces cerevisiae* replication and recombination defective mutants. *Nat. Genet.* 23:81–85.

Cheng, C., P. Fabrizio, H. Ge, V.D. Longo, and L.M. Li. 2007a. Inference of transcription modification in long-live yeast strains from their expression profiles. *BMC Genomics.* 8:219.

Cheng, C., P. Fabrizio, H. Ge, M. Wei, V.D. Longo, and L.M. Li. 2007b. Significant and systematic expression differentiation in long-lived yeast strains. *PLoS One.* 2:e1095.

DePinho, R.A. 2000. The age of cancer. *Nature.* 408:248–254.

Fabrizio, P., and V.D. Longo. 2003. The chronological life span of *Saccharomyces cerevisiae*. *Aging Cell.* 2:73–81.

Fabrizio, P., and V.D. Longo. 2007. The chronological life span of *Saccharomyces cerevisiae*. *Methods Mol. Biol.* 371:89–95.

Fabrizio, P., F. Pozza, S.D. Pletcher, C.M. Gendron, and V.D. Longo. 2001. Regulation of longevity and stress resistance by Sch9 in yeast. *Science.* 292:288–290.

Fabrizio, P., L.L. Liou, V.N. Moy, A. Diaspro, J.S. Valentine, E.B. Gralla, and V.D. Longo. 2003. SOD2 functions downstream of Sch9 to extend longevity in yeast. *Genetics.* 163:35–46.

Fabrizio, P., L. Battistella, R. Vardavas, C. Gattazzo, L.L. Liou, A. Diaspro, J.W. Dossen, E.B. Gralla, and V.D. Longo. 2004. Superoxide is a mediator of an altruistic aging program in *Saccharomyces cerevisiae*. *J. Cell Biol.* 166:1055–1067.

Fabrizio, P., C. Gattazzo, L. Battistella, M. Wei, C. Cheng, K. McGrew, and V.D. Longo. 2005. Sir2 blocks extreme life-span extension. *Cell.* 123:655–667.

Gan, G.N., J.P. Wittschieben, B.O. Wittschieben, and R.D. Wood. 2008. DNA polymerase zeta (pol zeta) in higher eukaryotes. *Cell Res.* 18:174–183.

Gibbs, P.E., X.D. Wang, Z. Li, T.P. McManus, W.G. McGregor, C.W. Lawrence, and V.M. Maher. 2000. The function of the human homolog of *Saccharomyces cerevisiae* REV1 is required for mutagenesis induced by UV light. *Proc. Natl. Acad. Sci. USA.* 97:4186–4191.

Grollman, A.P., and M. Moriya. 1993. Mutagenesis by 8-oxoguanine: an enemy within. *Trends Genet.* 9:246–249.

Haracska, L., I. Unk, R.E. Johnson, E. Johansson, P.M. Burgers, S. Prakash, and L. Prakash. 2001. Roles of yeast DNA polymerases delta and zeta and of Rev1 in the bypass of abasic sites. *Genes Dev.* 15:945–954.

Haracska, L., S. Prakash, and L. Prakash. 2002. Yeast Rev1 protein is a G template-specific DNA polymerase. *J. Biol. Chem.* 277:15546–15551.

Heidenreich, E., and U. Wintersberger. 1998. Replication-dependent and selection-induced mutations in respiration-competent and respiration-deficient strains of *Saccharomyces cerevisiae*. *Mol. Gen. Genet.* 260:395–400.

Heidenreich, E., R. Novotny, B. Kneidinger, V. Holzmann, and U. Wintersberger. 2003. Non-homologous end joining as an important mutagenic process in cell cycle-arrested cells. *EMBO J.* 22:2274–2283.

Hlavatá, L., and T. Nyström. 2003. Ras proteins control mitochondrial biogenesis and function in *Saccharomyces cerevisiae*. *Folia Microbiol. (Praha).* 48:725–730.

Houtgraaf, J.H., J. Versmissen, and W.J. van der Giessen. 2006. A concise review of DNA damage checkpoints and repair in mammalian cells. *Cardiovasc. Revasc. Med.* 7:165–172.

Johnson, R.E., M.T. Washington, S. Prakash, and L. Prakash. 1999. Bridging the gap: a family of novel DNA polymerases that replicate faulty DNA. *Proc. Natl. Acad. Sci. USA.* 96:12224–12226.

Kobayashi, S., M.R. Valentine, P. Pham, M. O'Donnell, and M.F. Goodman. 2002. Fidelity of *Escherichia coli* DNA polymerase IV. Preferential generation of small deletion mutations by dNTP-stabilized misalignment. *J. Biol. Chem.* 277:34198–34207.

Kovtun, I.V., Y. Liu, M. Bjoras, A. Klungland, S.H. Wilson, and C.T. McMurray. 2007. OGG1 initiates age-dependent CAG trinucleotide expansion in somatic cells. *Nature.* 447:447–452.

Kozmin, S.G., Y.I. Pavlov, T.A. Kunkel, and E. Sage. 2003. Roles of *Saccharomyces cerevisiae* DNA polymerases Poleta and Polzeta in response to irradiation by simulated sunlight. *Nucleic Acids Res.* 31:4541–4552.

Kreutzer, D.A., and J.M. Essigmann. 1998. Oxidized, deaminated cytosines are a source of C —> T transitions in vivo. *Proc. Natl. Acad. Sci. USA.* 95:3578–3582.

Lawrence, C.W. 2004. Cellular functions of DNA polymerase zeta and Rev1 protein. *Adv. Protein Chem.* 69:167–203.

Le Page, F., A. Margot, A.P. Grollman, A. Sarasin, and A. Gentil. 1995. Mutagenicity of a unique 8-oxoguanine in a human Ha-ras sequence in mammalian cells. *Carcinogenesis.* 16:2779–2784.

Löbrich, M., and P.A. Jeggo. 2007. The impact of a negligent G2/M checkpoint on genomic instability and cancer induction. *Nat. Rev. Cancer.* 7:861–869.

Lombard, D.B., K.F. Chua, R. Mostoslavsky, S. Franco, M. Gostissa, and F.W. Alt. 2005. DNA repair, genome stability, and aging. *Cell.* 120:497–512.

Longo, V.D. 2003. The Ras and Sch9 pathways regulate stress resistance and longevity. *Exp. Gerontol.* 38:807–811.

Longo, V.D., and C.E. Finch. 2003. Evolutionary medicine: from dwarf model systems to healthy centenarians? *Science.* 299:1342–1346.

Longo, V.D., M.R. Lieber, and J. Vijg. 2008. Turning anti-ageing genes against cancer. *Nat. Rev. Mol. Cell Biol.* 9:903–910.

Madia, F., C. Gattazzo, P. Fabrizio, and V.D. Longo. 2007. A simple model system for age-dependent DNA damage and cancer. *Mech. Ageing Dev.* 128:45–49.

Madia, F., C. Gattazzo, M. Wei, P. Fabrizio, W.C. Burhans, M. Weinberger, A. Galbani, J.R. Smith, C. Nguyen, S. Huey, et al. 2008. Longevity mutation in SCH9 prevents recombination errors and premature genomic instability in a Werner/Bloom model system. *J. Cell Biol.* 180:67–81.

McKenzie, G.J., P.L. Lee, M.J. Lombardo, P.J. Hastings, and S.M. Rosenberg. 2001. SOS mutator DNA polymerase IV functions in adaptive mutation and not adaptive amplification. *Mol. Cell.* 7:571–579.

Minesinger, B.K., A.L. Abdulovic, T.M. Ou, and S. Jinks-Robertson. 2006. The effect of oxidative metabolism on spontaneous Pol zeta-dependent translesion synthesis in *Saccharomyces cerevisiae*. *DNA Repair (Amst.).* 5:226–234.

Moraes, E.C., S.M. Keyse, and R.M. Tyrrell. 1990. Mutagenesis by hydrogen peroxide treatment of mammalian cells: a molecular analysis. *Carcinogenesis.* 11:283–293.

Moriya, M. 1993. Single-stranded shuttle phagemid for mutagenesis studies in mammalian cells: 8-oxoguanine in DNA induces targeted G.C—>T.A transversions in simian kidney cells. *Proc. Natl. Acad. Sci. USA.* 90: 1122–1126.

Nelson, J.R., C.W. Lawrence, and D.C. Hinkle. 1996. Deoxycytidyl transferase activity of yeast REV1 protein. *Nature.* 382:729–731.

Nelson, J.R., P.E. Gibbs, A.M. Nowicka, D.C. Hinkle, and C.W. Lawrence. 2000. Evidence for a second function for *Saccharomyces cerevisiae* Rev1p. *Mol. Microbiol.* 37:549–554.

Ohmori, H., E.C. Friedberg, R.P. Fuchs, M.F. Goodman, F. Hanaoka, D. Hinkle, T.A. Kunkel, C.W. Lawrence, Z. Livneh, T. Nohmi, et al. 2001. The Y-family of DNA polymerases. *Mol. Cell.* 8:7–8.

Pagès, V., R.E. Johnson, L. Prakash, and S. Prakash. 2008. Mutational specificity and genetic control of replicative bypass of an abasic site in yeast. *Proc. Natl. Acad. Sci. USA.* 105:1170–1175.

Pedruzzi, I., N. Bürckert, P. Egger, and C. De Virgilio. 2000. *Saccharomyces cerevisiae* Ras/cAMP pathway controls post-diauxic shift element-dependent transcription through the zinc finger protein Gis1. *EMBO J.* 19:2569–2579.

Pinkston, J.M., D. Garigan, M. Hansen, and C. Kenyon. 2006. Mutations that increase the life span of *C. elegans* inhibit tumor growth. *Science.* 313:971–975.

Pollak, M.N., E.S. Schernhammer, and S.E. Hankinson. 2004. Insulin-like growth factors and neoplasia. *Nat. Rev. Cancer.* 4:505–518.

Prakash, S., R.E. Johnson, M.T. Washington, L. Haracska, C.M. Kondratick, and L. Prakash. 2000. Role of yeast and human DNA polymerase eta in error-free replication of damaged DNA. *Cold Spring Harb. Symp. Quant. Biol.* 65:51–59.

Prakash, S., R.E. Johnson, and L. Prakash. 2005. Eukaryotic translesion synthesis DNA polymerases: specificity of structure and function. *Annu. Rev. Biochem.* 74:317–353.

Quah, S.K., R.C. von Borstel, and P.J. Hastings. 1980. The origin of spontaneous mutation in *Saccharomyces cerevisiae*. *Genetics.* 96:819–839.

Rodriguez-Viciana, P., P.H. Warne, R. Dhand, B. Vanhaesebroeck, I. Gout, M.J. Fry, M.D. Waterfield, and J. Downward. 1994. Phosphatidylinositol-3-OH kinase as a direct target of Ras. *Nature.* 370:527–532.

Rodriguez-Viciana, P., O. Tetsu, K. Oda, J. Okada, K. Rauen, and F. McCormick. 2005. Cancer targets in the Ras pathway. *Cold Spring Harb. Symp. Quant. Biol.* 70:461–467.

Sabbioneda, S., I. Bortolomai, M. Giannattasio, P. Plevani, and M. Muzi-Falconi. 2007. Yeast Rev1 is cell cycle regulated, phosphorylated in response to DNA damage and its binding to chromosomes is dependent upon MEC1. *DNA Repair (Amst.).* 6:121–127.

Shen, W.H., A.S. Balajee, J. Wang, H. Wu, C. Eng, P.P. Pandolfi, and Y. Yin. 2007. Essential role for nuclear PTEN in maintaining chromosomal integrity. *Cell.* 128:157–170.

Skeen, J.E., P.T. Bhaskar, C.C. Chen, W.S. Chen, X.D. Peng, V. Nogueira, A. Hahn-Windgassen, H. Kiyokawa, and N. Hay. 2006. Akt deficiency impairs normal cell proliferation and suppresses oncogenesis in a p53-independent and mTORC1-dependent manner. *Cancer Cell.* 10:269–280.

Tang, M., P. Pham, X. Shen, J.S. Taylor, M. O'Donnell, R. Woodgate, and M.F. Goodman. 2000. Roles of *E. coli* DNA polymerases IV and V in lesion-targeted and untargeted SOS mutagenesis. *Nature.* 404:1014–1018.

Toda, T., S. Cameron, P. Sass, and M. Wigler. 1988. *SCH9*, a gene of *Saccharomyces cerevisiae* that encodes a protein distinct from, but functionally and structurally related to, cAMP-dependent protein kinase catalytic subunits. *Genes Dev.* 2:517–527.

Toker, A., and M. Yoeli-Lerner. 2006. Akt signaling and cancer: surviving but not moving on. *Cancer Res.* 66:3963–3966.

Urban, J., A. Soulard, A. Huber, S. Lippman, D. Mukhopadhyay, O. Deloche, V. Wanke, D. Anrather, G. Ammerer, H. Riezman, et al. 2007. Sch9 is a major target of TORC1 in *Saccharomyces cerevisiae*. *Mol. Cell.* 26:663–674.

Vergara, M., M. Smith-Wheelock, J.M. Harper, R. Sigler, and R.A. Miller. 2004. Hormone-treated snell dwarf mice regain fertility but remain long lived and disease resistant. *J. Gerontol. A Biol. Sci. Med. Sci.* 59:1244–1250.

Vijg, J. 2008. The role of DNA damage and repair in aging: new approaches to an old problem. *Mech. Ageing Dev.* 129:498–502.

Wang, Z. 2006. Controlled expression of recombinant genes and preparation of cell-free extracts in yeast. *Methods Mol. Biol.* 313:317–331.

Wang, D., D.A. Kreutzer, and J.M. Essigmann. 1998. Mutagenicity and repair of oxidative DNA damage: insights from studies using defined lesions. *Mutat. Res.* 400:99–115.

Washington, M.T., R.E. Johnson, S. Prakash, and L. Prakash. 1999. Fidelity and processivity of *Saccharomyces cerevisiae* DNA polymerase eta. *J. Biol. Chem.* 274:36835–36838.

Waters, L.S., and G.C. Walker. 2006. The critical mutagenic translesion DNA polymerase Rev1 is highly expressed during G(2)/M phase rather than S phase. *Proc. Natl. Acad. Sci. USA.* 103:8971–8976.

Waters, L.S., B.K. Minesinger, M.E. Wiltrout, S. D'Souza, R.V. Woodruff, and G.C. Walker. 2009. Eukaryotic translesion polymerases and their roles and regulation in DNA damage tolerance. *Microbiol. Mol. Biol. Rev.* 73:134–154.

Wei, M., P. Fabrizio, J. Hu, H. Ge, C. Cheng, L. Li, and V.D. Longo. 2008. Life span extension by calorie restriction depends on Rim15 and transcription factors downstream of Ras/PKA, Tor, and Sch9. *PLoS Genet.* 4:e13.

Wei, M., P. Fabrizio, F. Madia, J. Hu, H. Ge, L.M. Li, and V.D. Longo. 2009. Tor1/Sch9-regulated carbon source substitution is as effective as calorie restriction in life span extension. *PLoS Genet.* 5:e1000467.

Weinberger, M., L. Feng, A. Paul, D.L. Smith Jr., R.D. Hontz, J.S. Smith, M. Vujcic, K.K. Singh, J.A. Huberman, and W.C. Burhans. 2007. DNA replication stress is a determinant of chronological lifespan in budding yeast. *PLoS One.* 2:e748.